



Cite this article: Ponsiglione AM, Russo M, Netti PA, Torino E. 2016 Impact of biopolymer matrices on relaxometric properties of contrast agents. *Interface Focus* **6**: 20160061. <http://dx.doi.org/10.1098/rsfs.2016.0061>

One contribution of 12 to a theme issue 'Multifunctional nanostructures for diagnosis and therapy of diseases'.

Subject Areas:

bioengineering, biomaterials, nanotechnology

Keywords:

magnetic resonance imaging, contrast agents, hydrogels, relaxivity, water interface

Author for correspondence:

Enza Torino

e-mail: enza.torino@iit.it

Electronic supplementary material is available online at <http://dx.doi.org/10.6084/m9.figshare.c.3493035>.

Impact of biopolymer matrices on
relaxometric properties of contrast agents

Alfonso Maria Ponsiglione^{1,3}, Maria Russo^{1,3}, Paolo Antonio Netti^{1,2,3}
and Enza Torino^{2,3}

¹Department of Chemical, Materials and Production Engineering, and ²Interdisciplinary Research Center on Biomaterials, University of Naples Federico II, Piazzale V. Tecchio 80, 80125 Naples, Italy

³Center for Advanced Biomaterials for Healthcare IIT@CRIB, Istituto Italiano di Tecnologia, Largo Barsanti e Matteucci 53, 80125 Naples, Italy

ET, 0000-0002-8905-1925

Properties of water molecules at the interface between contrast agents (CAs) for magnetic resonance imaging and macromolecules could have a valuable impact on the effectiveness of metal chelates. Recent studies, indeed, demonstrated that polymer architectures could influence CAs' relaxivity by modifying the correlation times of the metal chelate. However, an understanding of the physico-chemical properties of polymer/CA systems is necessary to improve the efficiency of clinically used CAs, still exhibiting low relaxivity. In this context, we investigate the impact of hyaluronic acid (HA) hydrogels on the relaxometric properties of Gd-DTPA, a clinically used CA, to understand better the determining role of the water, which is crucial for both the relaxation enhancement and the polymer conformation. To this aim, water self-diffusion coefficients, thermodynamic interactions and relaxometric properties of HA/Gd-DTPA solutions are studied through time-domain NMR relaxometry and isothermal titration calorimetry. We observed that the presence of Gd-DTPA could alter the polymer conformation and the behaviour of water molecules at the HA/Gd-DTPA interface, thus modulating the relaxivity of the system. In conclusion, the tunability of hydrogel structures could be exploited to improve magnetic properties of metal chelates, inspiring the development of new CAs as well as metallopolymer complexes with applications as sensors and memory devices.

1. Introduction

Investigation of water molecules at the interface between relevant clinical contrast agents (CAs) for magnetic resonance imaging (MRI) and macromolecules can be of great interest to increase the performances of metal chelates. Indeed, most of the clinically used CAs are characterized by poor effectiveness in the high magnetic fields region (3 T and above), which is clinically favoured because of its higher signal-to-noise ratio and high-resolution imaging. MRI CAs also lack tissue specificity and can cause severe allergic effects, serious nephrotoxicity [1–3] and intracranial deposition of metal ion after repeated intravenous administration [4].

MRI performances of the CAs are well described by the 'relaxivity', defined as the rate of change in longitudinal or transverse relaxation times of the water protons per millimolar concentration of metal ions and determining the enhancement of the image contrast [5].

Despite their wide use, currently available CAs exhibit low relaxivity, which is far below its theoretical maximum required to obtain an accurate diagnosis at safe administration dosage [6]. In these perspectives, the possibility to have a CA that could work at low concentration but without giving over its signal intensity and, therefore, positive contrast effect is of great interest.

The extensive research on nano-engineered systems and polymer-based nanocomposites [7–17] has led to significant advances also in the field of MRI [13,18–22]. In particular, some recent studies have shown that nanoconstructs can improve CAs' relaxivity and many efforts have been devoted to the

development of polymer-based carriers for MRI CAs with particular reference to Gadolinium (Gd) chelates, which are the most commonly clinically used agents [18,23–28].

In this framework, Port *et al.* [29] have reported that the rigidification of MRI CAs, obtained through covalent or non-covalent binding to macromolecules, could be favourable to an increase in relaxivity of the metal chelate. Later, Decuzzi *et al.* [5,30] have proved that it is possible to modify, through the geometrical confinement, the magnetic properties of MRI CAs by controlling their characteristic correlation times without the chemical modification of the chelate structure. Furthermore, Courant *et al.* [25] have highlighted the capability of combined hydrogels to boost the relaxivity of Gd-based CAs. In detail, hydrogels [31–34] show three-dimensional networks, made of hydrophilic polymer chains held together by chemical or physical cross-linking; they are glassy in the dry state but have the ability to swell in water, forming elastic gels that retain a large quantity of fluid in their mesh-like structures [35]. The presence of hydrophilic polymer interfaces and the control of water behaviour in hydrogels play a fundamental role in the relaxation enhancement of the Gadolinium-based CAs by influencing the characteristic correlation times defined by the Solomon–Bloembergen–Morgan theory [36].

Despite several experimental studies addressed in this field, a comprehensive knowledge of the mechanisms involved in the relaxation enhancement due to the entrapment of CAs in polymer-based architectures is still missing. In particular, the role played by the water at the interface between polymer chains and MRI CAs has not been fully investigated and could lead to the availability of tailored models that accurately describe these novel complex systems.

In this perspective, we believe that a more in-depth knowledge about the interference between macromolecules and MRI CAs and an understanding of their physico-chemical properties is necessary to impact on the design strategies of the nanostructures and, consequently, to overcome the limitations of clinically used MRI CAs, particularly linked to the low relaxivity. To this aim, it is crucial to study the main phenomena involved in the formation of polymer matrices and how their properties can influence the relaxivity of MRI CAs.

In particular, this paper investigates the impact of hydrogel-CA systems on the relaxometric properties of metal chelates to understand clearly the role of the water, which mediates interactions and could be responsible for their behaviour in solution. Indeed, water is crucial both in the relaxation process and in the polymer conformation. On the one hand, the magnetic properties of the water protons surrounding the CA are fundamental to enhance the CA's relaxivity. On the other, the presence of water molecules can induce changes in the polymer structure through polar interactions, hydrogen bonding and osmotic pressure.

Among different biopolymers, hyaluronic acid (HA) [37] is chosen as a model polymer due to its hydrophilic nature and established biocompatibility and biodegradability. Commercially available Gd-DTPA is selected as the CA due to its widespread use in clinical practice [38]. It is worth highlighting that both the selected polymer and CA are FDA approved and clinically used products [1,39,40].

The first experiments are focused on determining the water self-diffusion coefficients in polymer and CA solutions through time-domain NMR relaxometry to observe changes in water mobility in the presence of both HA and Gd-DTPA. Self-diffusion measurements have already proved especially successful for

probing interfacial water structure and dynamics near various biological and polymer surfaces [41]. Intramolecular interactions, as well as entropy costs, can alter the mobility of solvent molecules within polymer matrices or in confined environments, with a slowing effect on the diffusion [42–44]. Moreover, since the relaxation efficiency is mediated by translational and rotational diffusion [41], a variation of the water diffusion behaviour at the interface between polymer chains and MRI CAs could impact on the characteristic correlation time, in particular the diffusion correlation time τ_D of the complex, thereby influencing the relaxometric properties of the metal chelate.

After that, isothermal titration calorimetry (ITC) is employed to investigate thermodynamic interactions involved in the mixing of HA with Gd-DTPA. As already reported elsewhere [45], molecular interactions are accompanied by some level of heat exchange between the interacting system and its surrounding medium, which can be evaluated at a constant temperature through the ITC technique. Therefore, to investigate interactions between HA and Gd-DTPA, titration experiments are performed using a Nano ITC Low Volume calorimeter (TA Instruments). Basic principles of ITC measurements have been widely discussed elsewhere [45–47].

Finally, relaxometric properties of HA/Gd-DTPA solutions are investigated by means of time-domain NMR relaxometry. The characterization of these systems, obtained through the combination of commercial MRI CAs and hydrophilic biopolymers, could give an insight into the development of novel hydrogel-based CAs without modifying the chemical structure or altering the biocompatibility of the original CA.

2. Material and methods

2.1. Materials

HA (Bohus Biotech, Sweden) with an average molecular weight of 42 000 Da is used for the polymer matrix because of its biocompatibility, biodegradability and swelling properties. Commercially available Gd-DTPA (Sigma-Aldrich) with a molecular weight of 547.57 Da is used since it is a well-known, low-risk CA. Divinyl sulfone (DVS) (Sigma-Aldrich) with a molecular weight of 118.15 Da is used as cross-linking agent. Milli-Q water is systematically used for sample preparation and analysis.

2.2. Sample preparation

Non-cross-linked hydrogel-CA solutions are prepared by dispersing both the HA and the Gd-DTPA powders in distilled deionized water and then mixing using a magnetic stirrer. Different HA concentrations, ranging from 0.1 to 5% w/v, are used for the experimentation. For each fixed concentration of HA, Gd-DTPA concentration is varied between 0 and 0.2 mM.

Cross-linked hydrogel-CA solutions are prepared by adding DVS to the above-described solutions to cross-link the polymer network chemically. Hydrogels are prepared at different HA : DVS ratios (from 1 : 1 to 1 : 16). The biocompatibility of HA–DVS hydrogels is already confirmed in the literature [48].

2.3. Water self-diffusion coefficient

Diffusion measurements of water molecules are carried out on a Bruker Minispec (mq 20) bench-top relaxometer operating at 20 MHz for protons (magnetic field strength: 0.47 T). A pulsed field gradient spin echo (PFG-SE) sequence [49], with two magnetic field gradient pulses of length δ and strength g , and with a delay Δ between the leading edges of them, is used to measure water self-diffusion coefficients. The self-diffusion coefficient, D ,

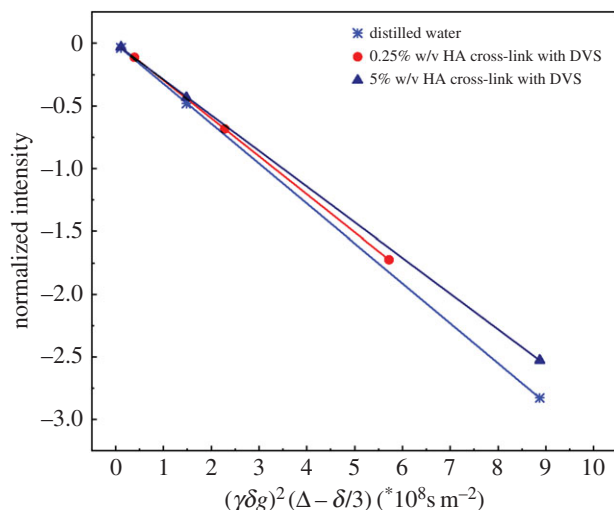


Figure 1. Stejskal–Tanner plot is used for calculating water self-diffusion coefficient of: (1) distilled water, (2) 0.25% w/v HA solution with 5 μl DVS 8 hours after the cross-linking reaction and (3) 5% w/v HA solution with 40 μl DVS 8 hours after the cross-linking reaction.

is derived by linear regression of signal attenuation ratio curve, a semi-logarithmic plot of the echo attenuation as a function of the tunable parameter of the sequence, $k = (\gamma\delta g)^2 \times (\Delta - \delta/3)$.

2.4. Isothermal titration calorimetry

ITC measurements are conducted by filling the sample cell (0.7 ml in volume) with an aqueous solution of HA at different concentrations (from 0.1 to 0.7% w/v) and the 50 μl syringe with an aqueous solution of Gd-DTPA at 1.5 mM. Measurements are performed at 25°C and fixed stirring rate of 200 r.p.m. Fifty injections, each of 1 μl of Gd-DTPA, are delivered at intervals of 500 s. Data analysis and processing to provide ITC and enthalpy change, ΔH , profiles are carried out using the Nano-Analyze (TA instruments) and the Origin Pro 9.1 SRO software (OriginLab Corporation, USA).

2.5. Relaxometric measurement

Relaxation times are measured on a Bruker Minispec (mq 60) bench-top relaxometer operating at 60 MHz for protons (magnetic field strength: 1.41 T). The acquisitions are performed at 37°C and, before each measurement, the sample is placed into the NMR probe for about 15 min for thermal equilibration. Longitudinal relaxation times, T_1 , are determined by both saturation and inversion recovery pulse sequences. The relaxation recovery curves are fitted using a multi-exponential model. The solid line represents the linear regression and relaxivity values, r_1 , are calculated from its slope. The longitudinal relaxation rate values, R_1 , defined as the inverse of the longitudinal relaxation time, $R_1 = 1/T_1$, s^{-1} , are plotted versus each concentration of CA, measured in millimolar. Data are treated by a least-squares method using ORIGIN PRO v. 9.1 SRO software (OriginLab Corporation). Furthermore, the relaxation time distribution is obtained with the CONTIN algorithm. The relaxation spectrum is normalized with respect to the CONTIN processing parameters. Therefore, the integral of a peak corresponds to the contribution of the species exhibiting this peculiar relaxation to the relaxation time spectrum.

3. Results and discussion

3.1. Diffusion coefficient

In our systems, we have observed that water mobility slightly changes with increasing network density induced by cross-

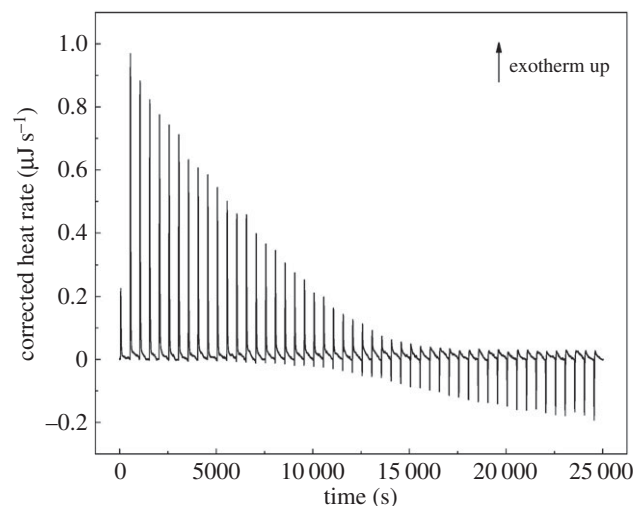


Figure 2. Thermogram (heat flow versus time) of Gd-DTPA into aqueous solution of HA at 0.6% w/v. Temperature and stirring rate have been kept constant at 25°C and 200 r.p.m., respectively.

Table 1. Range of water self-diffusion coefficients, D , measured for: (1) distilled water, (2) Gd-DTPA solutions at different Gd-DTPA concentrations, (3) 0.25 and 5% w/v HA hydrogel solutions at varying cross-linking degrees, i.e. different DVS concentrations.

HA (% w/v)	DVS (μl)	Gd-DTPA (mM)	D^a ($\times 10^{-9} \text{m}^2 \text{s}^{-1}$)
0	0	0	3.19
0	0	0.05 ÷ 1	3.18 ÷ 3.09
0.25	0 ÷ 25	0	3.05 ÷ 2.90
5	5 ÷ 40	0	2.88 ÷ 2.83

^aValues of the standard deviation for the measured diffusion coefficients are all below $0.4 \times 10^{-12} \text{m}^2 \text{s}^{-1}$.

linking reaction (figure 1). Besides, a more significant decrease in the water diffusion is observed in the presence of increasing polymer concentration rather than increasing CA concentration (table 1). However, the study of the diffusion coefficient as a function of the cross-linking degree requires further investigation to understand its influence on the relaxometric properties. Further details on diffusion data are reported in the electronic supplementary material, tables S1 and S2. Furthermore, results show that water mobility starts decreasing even at very low polymer concentration (0.25% w/v HA). This dynamic can be attributed to the high molecular weight and hydrophilicity of the HA, which allows the formation of several hydrogen bonds at the surface of the polymer, thereby stabilizing the polymer structure and reducing water self-diffusion.

3.2. Isothermal titration calorimetry

Here, ITC is proposed to calculate the energetic contribution and thermodynamic interactions deriving from the mixing of Gd-chelates with the polymer solution.

In our experiment, a simple dilution of Gd-DTPA in water or water in HA exhibits only small constant exothermic peaks (see the electronic supplementary material, figures S1 and S2). On the contrary, when Gd-DTPA is injected as titrant into the

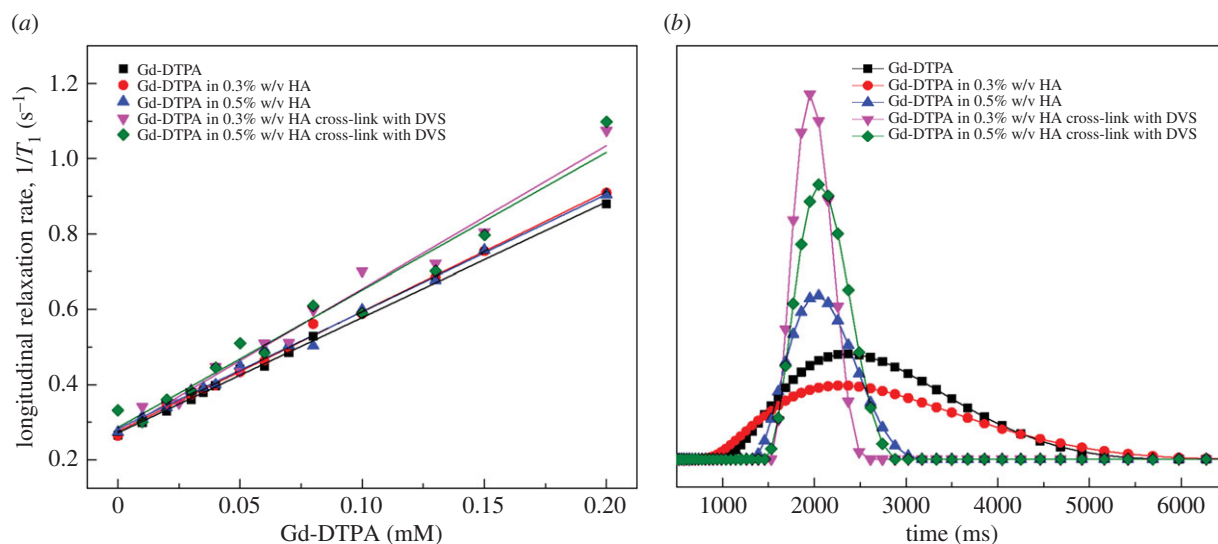


Figure 3. (a) Longitudinal relaxation rate as a function of Gd-DTPA concentration and (b) longitudinal relaxation time distribution for: (1) Gd-DTPA in distilled water, (2) Gd-DTPA in 0.3% w/v HA solution, (3) Gd-DTPA in 0.5% w/v HA solution, (4) Gd-DTPA in 0.3% w/v HA cross-linked with DVS (HA:DVS = 1 : 8) and (5) Gd-DTPA in 0.5% w/v HA cross-linked with DVS (HA:DVS = 1 : 8). Linear regression is applied to each set of data reported in (a).

cell containing HA solution a change from exothermic to endothermic behaviour is clearly observed. This change occurs at an HA/Gd-DTPA molar ratio of 0.5 (figure 2), i.e. when the molar concentration of Gd-DTPA in solution is twice the HA molar concentration. Starting from these observations, we hypothesize that at a certain HA/Gd-DTPA ratio, the enthalpy variations obtained in the binding experiment can be related to changes in the polymer structure, which in turn can be associated with the water-mediated interaction between the Gd-chelate and the polymer. The presence of Gd-DTPA, which has a high affinity for water molecules, may interfere with the polymer solution and induce peculiar arrangements in polymer chains' conformation.

These experimental observations could be of crucial importance in the design of polymer-based MRI CAs. Therefore, we have subsequently investigated how the polymer conformation can influence the relaxometric properties of the MRI complex in the polymer solution.

3.3. Time-domain relaxometry

Through time-domain relaxometry, relationships between system formulation, polymer matrices and relaxivity enhancement are provided. Results show how the relaxivity could be varied by changing the structural parameters of the hydrogel, namely polymer concentration and cross-linking degree (DVS concentration). Figure 3a,b displays the longitudinal relaxation rate, R_1 , and longitudinal relaxation time distribution for Gd-DTPA in distilled water and different cross-linked and non-cross-linked HA/Gd-DTPA solutions.

In detail, figure 3a demonstrates the variation of relaxation rates against the concentration of Gd-DTPA. As expected, R_1 rises linearly as Gd-DTPA concentration increases and surprisingly, the relaxivity, r_1 , appears to be tuned mostly by the variation of hydrogel structure (polymer concentration and cross-linking degree). Therefore, we found out that it could be possible to modulate the r_1 by changing the DVS concentration and to induce corresponding changes in the relaxation rates through the hydrogel matrix. Slopes of the regression lines in figure 3a, indicating each obtained relaxivity r_1 value, are reported in table 2.

Table 2. Relaxivity enhancement for the investigated polymer/CA systems.

HA (% w/v)	DVS (% w/v)	r_1 (mM ⁻¹ s ⁻¹)	r_1 increment (%)
0	0	3.07 ± 0.04	0
0.3	0	3.18 ± 0.05	3.6
0.3	2.4	3.81 ± 0.16	24.1
0.5	0	3.11 ± 0.06	1.3
0.5	4	3.65 ± 0.23	18.9
0.7	0	3.26 ± 0.06	6.2
0.7	5.6	3.41 ± 0.21	11.1

Figure 3b highlights, through the relaxation time distribution, the influence of hydrogel structure on the relaxation times as already discussed in figure 3a. In particular, it displays a narrower relaxation time distribution in the presence of cross-linking, thereby indicating an enhancement of the MRI signal.

As shown in table 2, a slight increase in the relaxivity (from 1 to 6%) on the reference solution (Gd-DTPA in water) is observed for the non-cross-linked samples. Besides, for cross-linked hydrogel-CA systems, in the presence of a cross-linked network, the relaxivity increases to an even greater extent, ranging from 11% up to 25%. About this last result, it seems that the cross-linking degree is interfering more on the relaxivity of CAs than on the diffusivity of water, acting, therefore, more on the rigidification of the CAs than on the water mobility. However, this aspect is of crucial importance and will require further investigations and comparisons.

Percentages of increment in the relaxivity are calculated by dividing the difference between the relaxivity of the cross-linked and non-cross-linked polymer/CA system and the reference (Gd-DTPA in water) by that of the reference solution, as follows:

$$r_1 \text{ increment} = \frac{1/T_1|_{\text{Gd-DTPA in HA}} - 1/T_1|_{\text{Gd-DTPA}}}{1/T_1|_{\text{Gd-DTPA}}} \times 100.$$

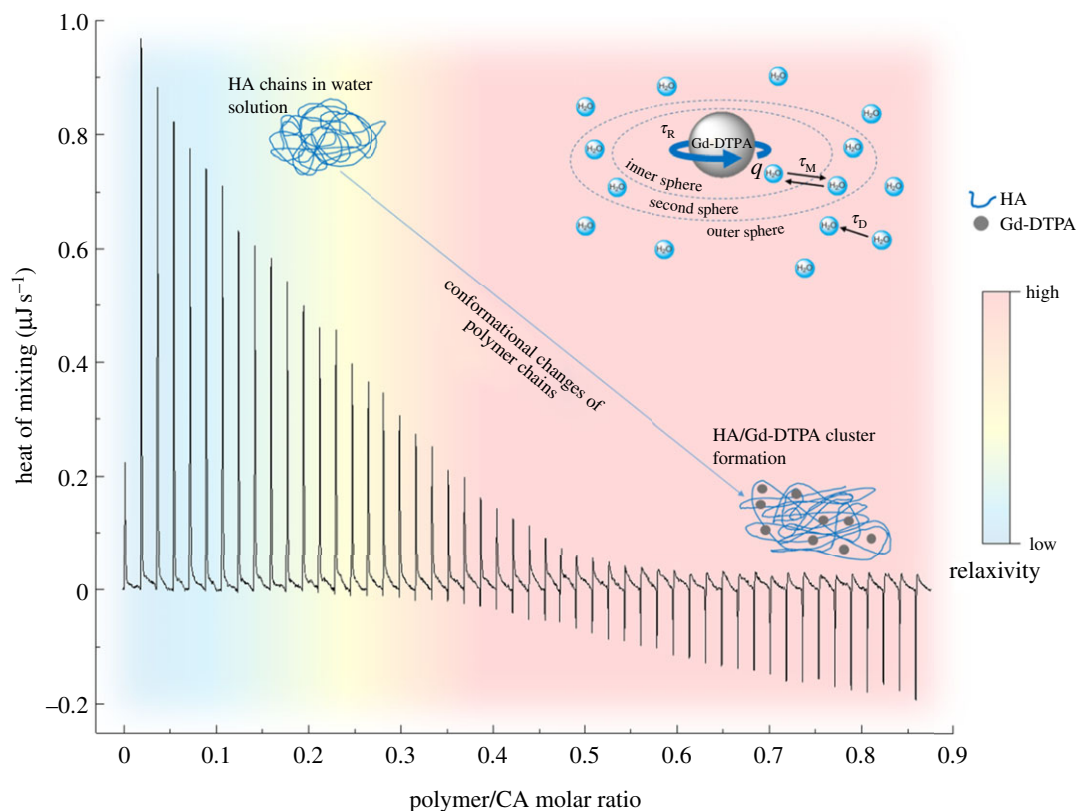


Figure 4. Relaxation rate enhancement induced by water-mediated HA/Gd-DTPA interactions.

For further details on relaxometric data, refer to the electronic supplementary material, table S3.

3.4. Theoretical interpretation of the enhanced relaxivity

Starting from the Solomon–Bloembergen–Morgan (SBM) theory [36], the physics of CAs is described by a set of physico-chemical parameters characterizing the fluctuating magnetic dipole created by the paramagnetic ion. In detail, according to the SBM model, the metal complex can be viewed as having separate coordination spheres [50]: the inner sphere (IS), which consists of water molecules directly coordinated to the metal ion, and the outer sphere (OS), which is a less-organized structure consisting of bulk water molecules diffusing in the near environment of the metal complex. In some cases, a second sphere (SS) contribution is taken into account, which is related to water molecules hydrogen bonded to the metal complex [51]. Each of the above-mentioned coordination spheres has its characteristic parameters. IS parameters include the number of labile water molecules coordinated to the metal ion (q), the residence time of the coordinated water molecule (τ_M), which in turn determines the rate of the coordinated water molecule exchanging with the bulk, and the rotational correlation time (τ_R), which is how quickly the contrast agent is tumbling in solution. Conversely, OS parameters include the translational diffusional time (τ_D), which represents the diffusion of water molecules in the bulk near to the Gd complex.

It is already known that molecular motion, size, rigidity and possible binding between Gd-chelates and other macromolecules may induce changes in relaxivity [2]. Furthermore, polymer architecture and properties can strongly affect the MRI enhancement [20,26,29].

As previously reported in the SBM theory, characteristic parameters of the metal chelate can be physically or chemically tuned and are of primary importance in the design of new CAs [52]. In particular, the Gd-chelator determines the number of coordinated water molecules (q) and the water exchange rate (k_{ex}), which is the inverse of the residence time τ_M . Moreover, decreased τ_D and τ_R , which can be obtained, for instance, through the binding of the metal chelate with large macromolecules, generally yield increased relaxation rates at low magnetic fields (less than 1.5 T) [3].

Our findings report that the presence of a polymer network can significantly affect the relaxation enhancement since it influences the hydration mechanism of the CA, i.e. the number of water molecules in either the IS, SS or OS, their diffusion behaviour and exchange rate with the water molecule coordinated to the metal ion.

Firstly, as a result of the diffusion measurements, we can observe that thanks to the high hydrophilicity of the HA promoting the hydrogen bonds formation at the surface of the polymer, water mobility starts decreasing even at very low polymer concentrations. Secondly, ITC results suggest that the presence of Gd-DTPA induces considerable thermodynamic variations in the polymer/CA mixing process that can be related to changes in polymer conformation. Finally, taking into consideration the computed relaxivity values, we can hypothesize that the hydrogel structure, which is strictly dependent on the water content and its dynamics within the polymer matrix, can significantly impact on the relaxivity of the whole polymer/CA system.

As schematically represented in figure 4, the obtained results suggest that changes in polymer conformation, induced by varying polymer/CA molar ratio, could be furtherly exploited to improve the relaxivity of the CA.

Indeed, the altered behaviour of the water molecules at the HA/Gd-DTPA interface, exhibiting reduced mobility

and strong interactions with the highly hydrophilic polymer surface, may have a considerable impact on the correlation times, especially τ_M and τ_D . In fact, the presence of polymer hydrophilic groups can change the access of bulk water molecules to the coordinated water molecule and, thus, alter the water exchange rate ($k_{ex} = 1/\tau_M$). Moreover, polymer chains can slightly reduce the mobility of the OS water molecules, with a consequent decreasing of τ_D . A simultaneous reduction of the CA's tumbling rate (τ_R) can also be hypothesized since the environment provided by the presence of the polymer chains as well as of the cross-linking degree may induce a slower rotation of the metal chelate.

4. Conclusion

Here, a study of the interactions involved in hydrogel-based CA solutions has been presented, aiming at understanding the key role of the water as a mediating agent that acts at the interface between the polymer and the metal chelate and determines both the polymer conformation and the relaxation enhancement.

The systems have been investigated by mixing cross-linked or non-cross-linked HA with Gd-DTPA at specific polymer/CA molar ratios in aqueous solution without introducing chemical modifications of the CA. Water self-diffusion coefficients, as well as proton longitudinal relaxation curves for different HA/Gd-DTPA solutions, have been measured. A thermodynamic investigation of the mixing process between HA and Gd-DTPA in water has also been conducted.

We have observed that, in the presence of a cross-linked matrix, it is possible to modulate the water content of the system and, therefore, the hydration of the CA, by adjusting the cross-linking degree of the hydrogel structure. In these conditions, a more stable polymer network can be obtained, promoting more efficient water-polymer and water-CA

interactions that boost the relaxivity to higher values. The cross-linking degree is proposed as an advanced tool to modulate the hydrogel network and its properties, enabling the tuning of the relaxometric properties.

These findings could be useful to deepen the knowledge of hydrogel-CA systems and to achieve an advanced comprehension of the fundamental mechanisms that rule the interaction between MRI CAs and hydrogel matrices, and are responsible for the relaxation enhancement. Further characterization studies and computational simulations are necessary to gain insight on the water behaviour within polymeric matrices in the presence of metal chelates and the potential impact that these structures can have on the relaxometric properties of clinically used CAs and, therefore, on the performance of MRI diagnosis. The knowledge of these complex systems could be scaled to nanoscale dimensions, inspiring the development of a new class of nanostructured MRI CAs with highly tunable relaxometric properties as well as the production of metallopolymer complexes or magnetic and conductive polymer-based materials with applications in areas such as sensors, memory devices, nanolithography and controlled release.

Data accessibility. The datasets supporting this article have been uploaded as part of the electronic supplementary material.

Authors' contributions. A.M.P. and M.R. contributed to the collection and interpretation of all the presented data. Moreover, they carried out the data analyses and drafted the manuscript. P.A.N. and E.T. participated in the conception and the design of the study, revised the work critically for important intellectual content and gave final approval of the version to be published. All authors read and approved the final manuscript and guarantee its accuracy and integrity.

Competing interests. We have no competing interests.

Funding. We have no funding to report.

Acknowledgements. Authors warmly thank Dr Annamaria Grimaldi and Franca De Sarno for technical assistance in sample preparation used in the self-diffusion measurements and Ernesto Forte for the initial introduction to the diffusion gradient techniques.

References

- Zhou Z, Lu ZR. 2013 Gadolinium-based contrast agents for magnetic resonance cancer imaging. *Wiley Interdisc. Rev. Nanomed. Nanobiotechnol.* **5**, 1–18. (doi:10.1002/wnan.1198)
- Caravan P. 2006 Strategies for increasing the sensitivity of gadolinium based MRI contrast agents. *Chem. Soc. Rev.* **35**, 512–523. (doi:10.1039/b510982p)
- Bruckman MA, Yu X, Steinmetz NF. 2013 Engineering Gd-loaded nanoparticles to enhance MRI sensitivity via T1 shortening. *Nanotechnology* **24**, 462001. (doi:10.1088/0957-4484/24/46/462001)
- McDonald RJ, McDonald JS, Kallmes DF, Jentoft ME, Murray DL, Thielen KR, Williamson EE, Eckel LJ. 2015 Intracranial gadolinium deposition after contrast-enhanced MR imaging. *Radiology* **275**, 772–782. (doi:10.1148/radiol.15150025)
- Sethi R *et al.* 2012 Enhanced MRI relaxivity of Gd³⁺-based contrast agents geometrically confined within porous nanoconstructs. *Contrast Media Mol. Imaging* **7**, 501–508. (doi:10.1002/cmmi.1480)
- Yang JJ *et al.* 2008 Rational design of protein-based MRI contrast agents. *J. Am. Chem. Soc.* **130**, 9260–9267. (doi:10.1021/ja800736h)
- Netti PA. 2014 Nano-engineered bioactive interfaces. *Interface Focus* **4**, 20130065. (doi:10.1098/rsfs.2013.0065)
- Wang X, He J, Wang Y, Cui F-Z. 2012 Hyaluronic acid-based scaffold for central neural tissue engineering. *Interface Focus* **2**, 278–291. (doi:10.1098/rsfs.2012.0016)
- Wu C, Chang J. 2012 Mesoporous bioactive glasses: structure characteristics, drug/growth factor delivery and bone regeneration application. *Interface Focus* **2**, 292–306. (doi:10.1098/rsfs.2011.0121)
- Ahearne M. 2014 Introduction to cell-hydrogel mechanosensing. *Interface Focus* **4**, 20130038. (doi:10.1098/rsfs.2013.0038)
- Fadeeva E, Deiwick A, Chichkov B, Schlie-Wolter S. 2014 Impact of laser-structured biomaterial interfaces on guided cell responses. *Interface Focus* **4**, 20130048. (doi:10.1098/rsfs.2013.0048)
- Bhowmik D, Chiranjibi CR, Tripathi K, Kumar KS. 2010 Nanomedicine—an overview. *Int. J. PharmTech Res.* **2**, 2143–2151.
- Lacroix L-M, Delpech F, Nayral C, Lachaize S, Chaudret B. 2013 New generation of magnetic and luminescent nanoparticles for *in vivo* real-time imaging. *Interface Focus* **3**, 20120103. (doi:10.1098/rsfs.2012.0103)
- Li H, LaBean TH, Leong KW. 2011 Nucleic acid-based nanoengineering: novel structures for biomedical applications. *Interface Focus* **1**, 702–724. (doi:10.1098/rsfs.2011.0040)
- Shen Y, Shrestha R, Ibricevic A, Gunsten SP, Welch MJ, Wooley KL, Brody SL, Taylor J-SA, Liu Y. 2013 Antisense peptide nucleic acid-functionalized cationic nanocomplex for *in vivo* mRNA detection. *Interface Focus* **3**, 20120059. (doi:10.1098/rsfs.2012.0059)
- Sierra-Martin B, Fernandez-Barbero A. 2015 Multifunctional hybrid nanogels for theranostic applications. *Soft Matter* **11**, 8205–8216. (doi:10.1039/c5sm01789k)

17. Raemdonck K, Demeester J, De Smedt S. 2009 Advanced nanogel engineering for drug delivery. *Soft Matter* **5**, 707–715. (doi:10.1039/b811923f)
18. Zhu W, Artemov D. 2011 Biocompatible blood pool MRI contrast agents based on hyaluronan. *Contrast Media Mol. Imaging* **6**, 61–68. (doi:10.1002/cmim.404)
19. Berezin MY. 2015 *Nanotechnology for biomedical imaging and diagnostics: from nanoparticle design to clinical applications*. New York, NY: Wiley.
20. Davies G-L, Kramberger I, Davis JJ. 2013 Environmentally responsive MRI contrast agents. *Chem. Commun.* **49**, 9704–9721. (doi:10.1039/c3cc44268c)
21. Masotti A *et al.* 2009 Synthesis and characterization of polyethylenimine-based iron oxide composites as novel contrast agents for MRI. *Magn. Reson. Mater. Phys. Biol. Med.* **22**, 77–87. (doi:10.1007/s10334-008-0147-x)
22. Corti M *et al.* 2008 Magnetic and relaxometric properties of polyethylenimine-coated superparamagnetic MRI contrast agents. *J. Magn. Magn. Mater.* **320**, E316–E319. (doi:10.1016/j.jmmm.2008.02.115)
23. Xiao Y, Xue R, You T, Li X, Pei F. 2015 A new biodegradable and biocompatible gadolinium (III)-polymer for liver magnetic resonance imaging contrast agent. *Magn. Reson. Imaging* **33**, 822–828. (doi:10.1016/j.mri.2015.03.002)
24. Jeong SY, Kim HJ, Kwak B-K, Lee H-Y, Seong H, Shin BC, Yuk SH, Hwang S-J, Cho SH. 2010 Biocompatible polyhydroxyethylaspartamide-based micelles with gadolinium for MRI contrast agents. *Nanoscale Res. Lett.* **5**, 1970–1976. (doi:10.1007/s11671-010-9734-7)
25. Courant T *et al.* 2012 Hydrogels incorporating GdDOTA: towards highly efficient dual T1/T2 MRI contrast agents. *Angew. Chem-Int. Edn* **51**, 9119–9122. (doi:10.1002/anie.201203190)
26. Li Y, Beija M, Laurent S, vander Elst L, Muller RN, Duong HT, Lowe AB, Davis TP, Boyer C. 2012 Macromolecular ligands for gadolinium MRI contrast agents. *Macromolecules* **45**, 4196–4204. (doi:10.1021/ma300521c)
27. Courant T *et al.* 2013 Biocompatible nanoparticles and gadolinium complexes for MRI applications. *C.R. Chim.* **16**, 531–539. (doi:10.1016/j.crci.2012.12.010)
28. Arosio P *et al.* 2013 Hybrid iron oxide-copolymer micelles and vesicles as contrast agents for MRI: impact of the nanostructure on the relaxometric properties. *J. Mater. Chem. B* **1**, 5317–5328. (doi:10.1039/c3tb00429e)
29. Port M, Raynal I, Elst LV, Muller RN, Diouy F, Ferroud C, Guy A. 2006 Impact of rigidification on relaxometric properties of a tricyclic tetraazatriacetic gadolinium chelate. *Contrast Media Mol. Imaging* **1**, 121–127. (doi:10.1002/cmim.99)
30. Ananta JS *et al.* 2010 Geometrical confinement of gadolinium-based contrast agents in nanoporous particles enhances T-1 contrast. *Nat. Nanotechnol.* **5**, 815–821. (doi:10.1038/nnano.2010.203)
31. Pasqui D, De Cagna M, Barbucci R. 2012 Polysaccharide-based hydrogels: the key role of water in affecting mechanical properties. *Polymers* **4**, 1517–1534. (doi:10.3390/polym4031517)
32. Oliveira RN, Rouze R, Quilty B, Alves GG, Soares GDA, Thire RMSM, McGuinness GB. 2014 Mechanical properties and *in vitro* characterization of polyvinyl alcohol-nano-silver hydrogel wound dressings. *Interface Focus* **4**, 20130049. (doi:10.1098/rsfs.2013.0049)
33. Manetti C, Casciani L, Pescosolido N. 2002 Diffusive contribution to permeation of hydrogel contact lenses: theoretical model and experimental evaluation by nuclear magnetic resonance techniques. *Polymer* **43**, 87–92. (doi:10.1016/s0032-3861(01)00559-6)
34. Pal K, Banthia AK, Majumdar DK. 2009 Polymeric hydrogels: characterization and biomedical applications. *Des. Monomers Polym.* **12**, 197–220. (doi:10.1163/156855509X436030)
35. Omidian H, Park K. 2008 Swelling agents and devices in oral drug delivery. *J. Drug Delivery Sci. Technol.* **18**, 83–93. (doi:10.1016/S1773-2247(08)50016-5)
36. Wood ML, Hardy PA. 1993 Proton relaxation enhancement. *J. Magn. Reson. Imaging* **3**, 149–156. (doi:10.1002/jmri.1880030127)
37. Necas J, Bartosikova L, Brauner P, Kolar J. 2008 Hyaluronic acid (hyaluronan): a review. *Veterinari Medicina* **53**, 397–411.
38. Lu Z-R, Mohs AM, Zong Y, Feng Y. 2006 Polydisulfide Gd(III) chelates as biodegradable macromolecular magnetic resonance imaging contrast agents. *Int. J. Nanomedicine* **1**, 31–40. (doi:10.2147/nano.2006.1.1.31)
39. Kasraie N, Oviatt HW, Clarke GD. 2011 On the use of molecular weight cutoff cassettes to measure dynamic relaxivity of novel gadolinium contrast agents: example using hyaluronic acid polymer complexes in phosphate-buffered saline. *Radiol. Res. Pract.* **2011**, 808795. (doi:10.1155/2011/808795)
40. Huang C-H, Tsourkas A. 2013 Gd-based macromolecules and nanoparticles as magnetic resonance contrast agents for molecular imaging. *Curr. Top. Med. Chem.* **13**, 411–421. (doi:10.2174/1568026611313040002)
41. Yoo H, Paranjli R, Pollack GH. 2011 Impact of hydrophilic surfaces on interfacial water dynamics probed with NMR spectroscopy. *J. Phys. Chem. Lett.* **2**, 532–536. (doi:10.1021/jz200057g)
42. Ori G, Villemot F, Viau L, Vioux A, Coasne B. 2014 Ionic liquid confined in silica nanopores: molecular dynamics in the isobaric-isothermal ensemble. *Mol. Phys.* **112**, 1350–1361. (doi:10.1080/00268976.2014.902138)
43. Ori G, Massobrio C, Pradel A, Ribes M, Coasne B. 2015 Structure and dynamics of ionic liquids confined in amorphous porous chalcogenides. *Langmuir* **31**, 6742–6751. (doi:10.1021/acs.langmuir.5b00982)
44. Chiessi E, Cavalieri F, Paradossi G. 2007 Water and polymer dynamics in chemically cross-linked hydrogels of poly(vinyl alcohol): a molecular dynamics simulation study. *J. Phys. Chem. B* **111**, 2820–2827. (doi:10.1021/jp0671143)
45. Kabiri M, Unsworth LD. 2014 Application of isothermal titration calorimetry for characterizing thermodynamic parameters of biomolecular interactions: peptide self-assembly and protein adsorption case studies. *Biomacromolecules* **15**, 3463–3473. (doi:10.1021/bm5004515)
46. Martinez JC, Murciano-Calles J, Cobos ES, Iglesias-Bexiga M, Luque I, Ruiz-Sanz J. 2013 Isothermal titration calorimetry: thermodynamic analysis of the binding thermograms of molecular recognition events by using equilibrium models. In *Applications of calorimetry in a wide context: differential scanning calorimetry, isothermal titration calorimetry and microcalorimetry* (ed. AA Elkordy), chapter 4. INTECH Open Access. (doi:10.5772/53311)
47. Gouin S, Winnik FM. 2001 Quantitative assays of the amount of diethylenetriaminepentaacetic acid conjugated to water-soluble polymers using isothermal titration calorimetry and colorimetry. *Bioconjug. Chem.* **12**, 372–377. (doi:10.1021/bc000109w)
48. Oh EJ, Kang S-W, Kim B-S, Jiang G, Cho IH, Hahn SK. 2008 Control of the molecular degradation of hyaluronic acid hydrogels for tissue augmentation. *J. Biomed. Mater. Res. A* **86A**, 685–693. (doi:10.1002/jbm.a.31681)
49. Stejskal EO, Tanner JE. 1965 Spin diffusion measurements: spin echoes in the presence of a time-dependent field gradient. *J. Chem. Phys.* **42**, 288–292. (doi:10.1063/1.1695690)
50. Caravan P, Farrar CT, Frullano L, Uppal R. 2009 Influence of molecular parameters and increasing magnetic field strength on relaxivity of gadolinium- and manganese-based T₁ contrast agents. *Contrast Media Mol. Imaging* **4**, 89–100. (doi:10.1002/cmim.267)
51. Debroye E, Parac-Vogt TN. 2014 Towards polymetallic lanthanide complexes as dual contrast agents for magnetic resonance and optical imaging. *Chem. Soc. Rev.* **43**, 8178–8192. (doi:10.1039/c4cs00201f)
52. Hermann P, Kotek J, Kubicek V, Lukes I. 2008 Gadolinium(III) complexes as MRI contrast agents: ligand design and properties of the complexes. *Dalton Trans.* **52**, 3027–3047. (doi:10.1039/b719704g)